Short Article

Developmental Cell

Lipid Droplets Are Essential for Efficient Clearance of Cytosolic Inclusion Bodies

Highlights

- A microscopic screen in yeast uncovers 13 inclusion body resident proteins
- Iml2, an inclusion resident, is crucial for efficient clearance of inclusion bodies
- Iml2's interactors reveal a role for lipid droplets in inclusion clearance
- Lipid droplets produce a sterol derivative that assists in inclusion clearance

Authors

Ofer Moldavski, Triana Amen, ..., Daniel Kaganovich, Maya Schuldiner

Correspondence

dan@cc.huji.ac.il (D.K.), maya.schuldiner@weizmann.ac.il (M.S.)

In Brief

Inclusion bodies (IBs) house protein aggregates following protein folding stress, and their clearance post stress is poorly understood. Moldavski et al. identify in yeast the IB-associated protein Iml2 in connection with lipid droplets and IB clearance. They provide evidence that a sterol derivative from lipid droplets helps clear IBs.

Moldavski et al., 2015, Developmental Cell *33*, 1–8
June 8, 2015
http://dx.doi.org/10.1016/j.devcel.2015.04.015

CellPress

Please cite this article in press as: Moldavski et al., Lipid Droplets Are Essential for Efficient Clearance of Cytosolic Inclusion Bodies, Developmental Cell (2015), http://dx.doi.org/10.1016/j.devcel.2015.04.015

Developmental Cell
Short Article

Lipid Droplets Are Essential for Efficient Clearance of Cytosolic Inclusion Bodies

Ofer Moldavski,[1] Triana Amen,[2] Smadar Levin-Zaidman,[3] Miriam Eisenstein,[4] Ilana Rogachev,[5] Alexander Brandis,[5] Daniel Kaganovich,[2,*] and Maya Schuldiner[1,*]
[1]Department of Molecular Genetics, Weizmann Institute of Science, Rehovot 7610001, Israel
[2]Department of Cell and Developmental Biology, Alexander Silberman Institute of Life Sciences, Hebrew University of Jerusalem, Jerusalem 91904, Israel
[3]Electron Microscopy Unit, Weizmann Institute of Science, Rehovot 7610001, Israel
[4]Department of Chemical Research Support, Weizmann Institute of Science, Rehovot 7610001, Israel
[5]Department for Biological Services, Weizmann Institute of Science, Rehovot 7610001, Israel
*Correspondence: dan@cc.huji.ac.il (D.K.), maya.schuldiner@weizmann.ac.il (M.S.)
http://dx.doi.org/10.1016/j.devcel.2015.04.015

SUMMARY

Exposing cells to folding stress causes a subset of their proteins to misfold and accumulate in inclusion bodies (IBs). IB formation and clearance are both active processes, but little is known about their mechanism. To shed light on this issue, we performed a screen with over 4,000 fluorescently tagged yeast proteins for co-localization with a model misfolded protein that marks IBs during folding stress. We identified 13 proteins that co-localize to IBs. Remarkably, one of these IB proteins, the uncharacterized and conserved protein Iml2, exhibited strong physical interactions with lipid droplet (LD) proteins. Indeed, we here show that IBs and LDs are spatially and functionally linked. We further demonstrate a mechanism for IB clearance via a sterol-based metabolite emanating from LDs. Our findings therefore uncover a function for Iml2 and LDs in regulating a critical stage of cellular proteostasis.

INTRODUCTION

During stress, misfolded proteins can overload the capacities of the quality control machinery, forming aggregates and later accumulating in inclusion bodies (IBs). It has recently become clear that IB formation from aggregates (recently termed "stress foci" or "Q bodies") (Escusa-Toret et al., 2013; Spokoini et al., 2012) is an active cellular process (Kaganovich et al., 2008; Kopito, 2000). Moreover, the inability to clear aggregates from the cytosol, either by degradation or sequestration in IBs is toxic and underlies a number of human diseases (Amen and Kaganovich, 2015; Cohen et al., 2006). Recently, it has been demonstrated, in both yeast and mammals, that each IB has unique characteristics. (Kaganovich et al., 2008; Ogrodnik et al., 2014; Weisberg et al., 2012).

Although IBs have been studied extensively, we do not yet know the entire repertoire of IB resident proteins. Moreover, we have little insight into how IBs are formed during stress or cleared upon termination of stress. To address such questions, we visualized over 4,000 fluorescently tagged yeast proteins (Huh et al., 2003) to search for IB residents in a systematic and unbiased fashion and found 13 IB proteins, six of which are important for the efficient and rapid clearance of IBs after stress.

Focusing on a conserved yet unstudied protein that was essential for efficient inclusion clearance, Iml2, we demonstrate that it interacts with lipid droplet (LD) proteins. LDs are mainly known to function as storage compartments for non-polar lipids although some studies suggest their involvement in the degradation of specific proteins (Ohsaki et al., 2006). Here, we demonstrate a role for LDs in physically binding to, and clearing of, cytosolic IBs. We show that clearance is dependent on Iml2, the non-polar lipid steryl ester and a soluble sterol metabolite and suggest that this mechanism is conserved to mammals.

RESULTS AND DISCUSSION

To assemble a comprehensive list of IB resident proteins, we screened the yeast GFP library (Huh et al., 2003), a collection of ~4,000 strains in which GFP was integrated carboxy-terminally into the genomic locus of over 60% of yeast genes. To identify IBs with certainty, we co-localized each of the proteins with the IB marker, misfolded VHL tagged with mCherry (cherry-VHL) (Kaganovich et al., 2008; McClellan et al., 2005). To create a genetic background that causes a consistent misfolding stress, we used a hypomorphic allele of the 20S proteasome, *pup2-DAmP*, in which large IBs are formed (Figure S1A).

We introduced *cherry-VHL* and *pup2-DAmP* into the GFP library (Cohen and Schuldiner, 2011; Tong and Boone, 2006) and live-imaged all of the strains during logarithmic growth in galactose (to induce VHL expression) using a high content screening setup (Breker et al., 2013). Visual inspection of all strains yielded 13 GFP tagged proteins that co-localize with cherry-VHL: quality control components, translation and post-translational factors, and poorly characterized proteins (Figure 1A). Five of the quality control components were previously shown to localize with aggregates or IBs (Hill et al., 2014; Kaganovich et al., 2008; Malinovska et al., 2012; Specht et al., 2011), thus validating the screening platform. We verified the findings by visualizing the original GFP tagged strains during stress

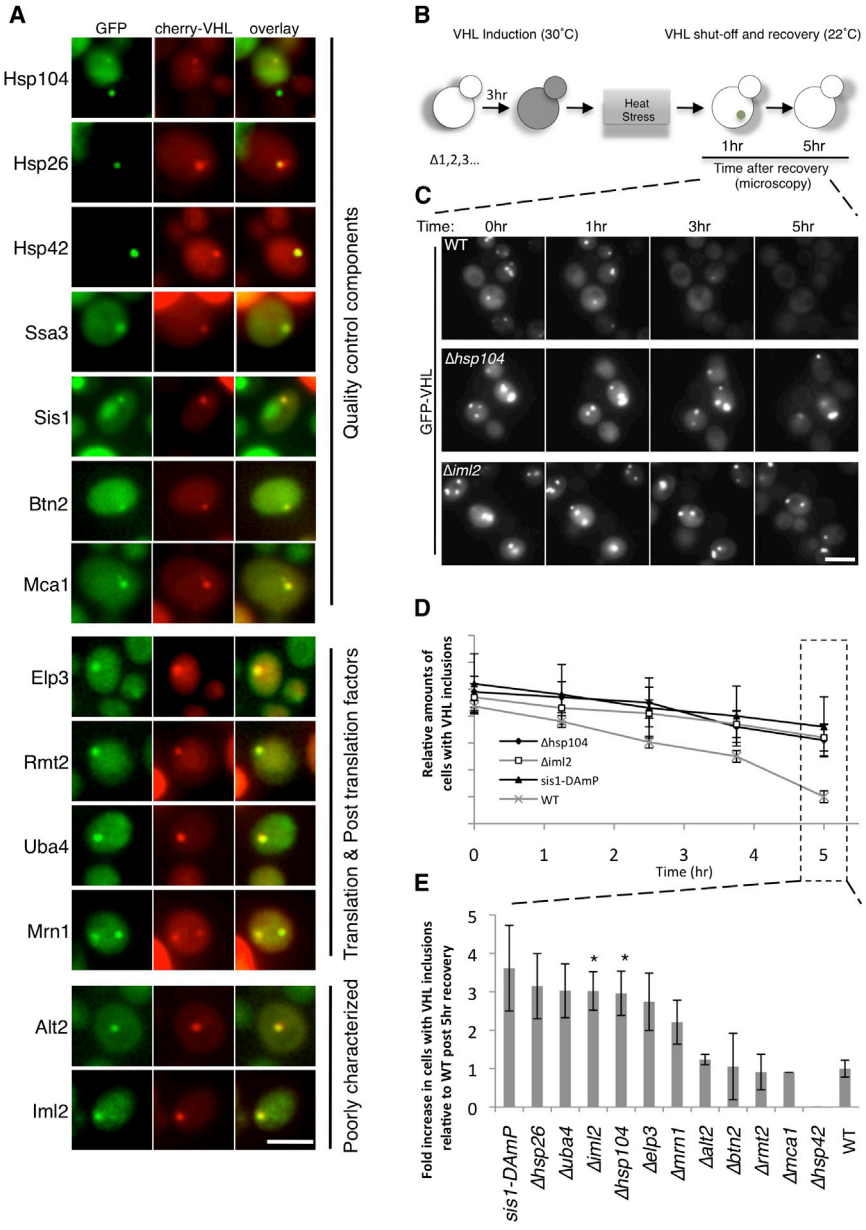

Figure 1. A Systematic Co-localization Screen Uncovers IB Residents

(A) Images of 13 GFP-tagged proteins that co-localize with *GALp-Cherry-VHL* in a *pup2-DAmP* background. The inclusion body (IB) residents can be divided into quality control components, translation and post-translation factors, and proteins whose function is poorly characterized.

(B) Schematic representation of the IB clearance assay.

(C) Representative images of time course to follow inclusion clearance in control (WT) strains and deletion strains (Δ*hsp104* and Δ*iml2*) that affect the process.

(D) Graph demonstrating that most strains had identical number of inclusions formed following stress. Since WT cells cleared IBs efficiently by 5 hr we chose this time point to represent in following figures.

(E) Bar graph of clearance rates in deletion strains of all identified IB residents 5 hr after exposure to stress conditions. Because *SIS1* is an essential gene, a hypomorphic allele (DAmP) was used in this assay. SE was calculated from three biological repeats, number of cells counted per strain per repeat: n = ±450 (p value < 0.05). Scale bar, 5 μm. See also Figure S1.

conditions (37°C for 90 min with proteasome inhibition) confirming IB residence (Figure S1B).

The presence of a protein in IBs could be due to two reasons—it could either function within the inclusion (machinery) or could be deposited there due to its misfolded conformation (substrate). As we are interested in machinery proteins, we wished to sieve out obvious substrates from our hit list. By screening our hits for proteins with substrate properties such as high turnover rate (Gardner et al., 2005), no affect on viability under stress, and localization changes that are dependent on ubiquitination, we found that the majority of our hits lack substrate properties. We could identify Alt2-GFP as a possible substrate (Figures S1C–S1F), which we find notable since there are few endogenous proteins characterized as misfolded quality control substrates.

To identify proteins that have a role in the clearance process, we followed the recovery of IBs post stress (37°C and proteasome inhibition) using time-lapse microscopy on deletions of the genes we found (excluding Δ*alt2*) (Figure 1B). At the first time point, both control (wild-type [WT]) and deletions had similar numbers of cells with IBs (except Δ*hsp42* that did not form IBs under these conditions) (Figure 1D), hence, most of the IB residents do not seem to affect the formation process. In WT cells, 5 hr following termination of stress, the majority of cells had cleared all cytosolic inclusions (Figure 1D). As expected, this was not the case for the deletion of the disaggregase *hsp104* in which IBs sustained 5 hr post stress (Spokoini et al., 2012), demonstrating that our assay gives a good indication of a protein's role in IB clearance (Figure 1C). When quantifying the relative percent of cells still harboring cytosolic inclusions five hours post stress, we found that seven of the deletions had a significant effect on clearance (Figure 1E). Three of the strains identified were chaperones (Hsp104, Hsp26, and Sis1) with prior evidence of their involvement in protein folding processes (Haslbeck et al., 2005; Malinovska et al., 2012; Parsell et al., 1994). However, the other four deletions were of genes with no prior connection to chaperone activity, IBs, or quality control.

Of particular interest was the uncharacterized protein Iml2. This protein is highly conserved from yeast to mammals (the human homolog is TetraTricopeptide Repeat Domain 39B/C,

TTC39B/C), and mutations in it are linked to several human diseases (Kuang et al., 1998; Teslovich et al., 2010). To validate Iml2 as a bona fide IB resident, we modeled it and found that it most likely is a soluble protein as expected from an IB resident (Figure S2A) (Karplus, 2009; Pettersen et al., 2004). Indeed, tagging with GFP at either termini demonstrated co-localization with IBs (Figure S2B). To ensure that the role of Iml2 is not specific to VHL, we measured the clearance of Alt2, the newly characterized endogenous quality control substrate, as well. Indeed, deletion of Iml2 resulted in a severe IB clearance defect for Alt2, confirming its affect on clearance is general (Figure S2C).

To understand the role of Iml2 in clearance, we performed a physical interaction screen by using a systematic protein complementation assay (Tarassov et al., 2008). We found that Iml2 interacts with two proteins, Pet10 and Pdr16 (Figure 2A) preferentially during stress when it is found solely in IBs. Interestingly, both identified interacting proteins are residents of lipid droplets (LDs) in line with previous high-throughput screens (Pu et al., 2011) (Figure 2A). To verify this interaction, we performed a pull-down of Iml2 and could detect an interaction with Pet10 specifically under stress conditions when Iml2 becomes an IB resident. As a control, the close homolog of Iml2, Ykr018c, did not bind to Pet10, assuring the specificity of Iml2's interaction (Figure 2B).

Since Iml2 binds LD proteins only under conditions where it is localized exclusively to IBs, this necessitates that LDs and IBs lie in close proximity during misfolding stress. Indeed, cells expressing Hsp104-GFP as an IB marker and Erg6-RFP as a LD marker demonstrate that under stress conditions many instances of proximity between IBs and LDs occur (Figure 2C) and could also be visualized by electron microscopy (Figure S2D). Time-lapse microscopy under stress conditions demonstrated IBs and LDs moving together in a correlated fashion (Figure 2D), indicative of a physical tethering between the compartments. The co-localization between the two compartments became even more apparent when visualizing a Δ*fld1* strain, which causes the LDs to cluster (Szymanski et al., 2007) (Figure 2E).

To further define the nature of this proximity, we constructed a strain carrying a split Venus reporter for the contact surface between LDs and IBs (Sung and Huh, 2007). Specifically, one-half of the fluorescent protein Venus was fused to the abundant IB marker, Hsp104, and the other to the LD marker, Faa4 (Huh et al., 2003). When co-expressed in the same cell under stress conditions we could identify a strong Venus signal. This signal was specific as the abundant cytosolic (non-IB) protein, Sem1, did not display a Venus signal (Figure S2E). Co-localization of the Venus foci with the LD marker, Erg6-cherry, shows that the contact between LDs and IBs occurs only with a subpopulation of LDs (Figure 2F, upper panel). Remarkably, the Venus foci is fully co-localized with Pdr16, an Iml2 interactor (Figure 2A), which is only expressed in one LD per cell and probably defines a certain functional subset of LDs (Ren et al., 2014) (Figure 2F, lower panel). Moreover, while Δ*iml2* and Δ*pet10* failed to impact proximity, loss of *PDR16* abolished the Venus signal (Figure 2G) demonstrating that the proximity is genetically regulated. However, the nature of the tethering force remains elusive and may either require tethering proteins or be indirect through the interactions of each structure with the ER. Nonetheless, this discovery prompted us to further explore the biological significance of the specific and regulated contact formed between IBs and LDs under stress conditions.

To test whether the LDs themselves have a role in IB clearance, we used a quadruple deletion strain (Δ*dga1*, Δ*lro1*, Δ*are1*, Δ*are2*) that completely lacks LDs (ΔLD) (Sandager et al., 2002). Indeed, this strain has an IB clearance defect similar in magnitude to Δ*iml2* (Figures 3A and 3B). We first verified that the IB clearance defect is not a by-product of reduced autophagy (Koenig et al., 2015; Li et al., 2015; Pfisterer et al., 2014; Spang et al., 2014) by deleting core autophagy genes (Δ*atg1*, Δ*atg2*, Δ*atg3*, Δ*atg8*) (data not shown). In an attempt to uncover the mechanism of the effect we screened a collection of mutants in all LD proteins (Table S1). Eight deletions were found to phenocopy the defect of the ΔLD strain (Figure 3C), three of which are proteins that interact with Iml2: Pdr16, Erg6, and Pet10, suggesting that the interaction with these three proteins is somehow required for LD-mediated IB clearance.

Because mutants in both *ERG6* and *PDR16* had defects in clearance, and since both are known to affect sterol metabolism (McCammon et al., 1984; van den Hazel et al., 1999), we tested whether the lipid composition of LDs affects the clearance of IBs. In LDs lipids are stored either as the sterol derivative steryl ester (STE) or the non-polar lipid triacylglycerol (TAG). Measuring IB clearance in two double deletion strains for the enzymes that are responsible for the biosynthesis of each type of storage lipid; Δ*dga1*, Δ*lro1* (that completely lacks TAGs, ΔTAG) and Δ*are1*, Δ*are2* (that completely lacks STE, ΔSTE) (Sandager et al., 2002) we saw that the ΔTAG strain cleared IBs as the control strain. However, the ΔSTE strain had a very severe defect in clearing IBs, (Figures 3D and S3A). Growth rates of these mutants were comparable (Figure S3B), as was the number and size of LDs (Figures S3C and S3D) suggesting that the difference in IB clearance capacity is not an indirect effect. The effect of STE deletion on IB clearance appears to be specific for two additional reasons. First, we could reduce the levels of STE by an alternate mechanism, overexpression of the STE hydrolase Yeh1 (Köffel et al., 2005), causing a similar loss of IB clearance (Figure 3D). Second, we tested dozens of mutants in all other lipid biosynthesis pathways and found no effects on IB clearance (Table S2) demonstrating that the phenotype of STE loss is not a general result of changes in lipid homeostasis in the cell.

Since STE are hydrophobic molecules, we hypothesized that they could act locally to solubilize hydrophobic interactions between aggregates inside IBs, acting as a detergent or a "chemical chaperone." An example for such a chemical chaperone is tauroursodeoxycholic acid (TUDCA), a sterol-based molecule with hydroxyl and Taurine groups, that alleviates folding stress in mammalian cell lines (de Almeida et al., 2007). According to this model, LDs may act as portable reservoirs for sterol-based solvents, delivering them to IBs when disaggregation, refolding, and clearance are required. This would also explain the requirement for physical proximity between the two compartments as transfer of a detergent like molecule must be local and regulated.

To determine whether such a soluble sterol metabolite, indeed, exists in yeast, we performed a non-targeted lipid profiling approach to assess differences in lipid species between a WT strain grown under stress or non-stress conditions.

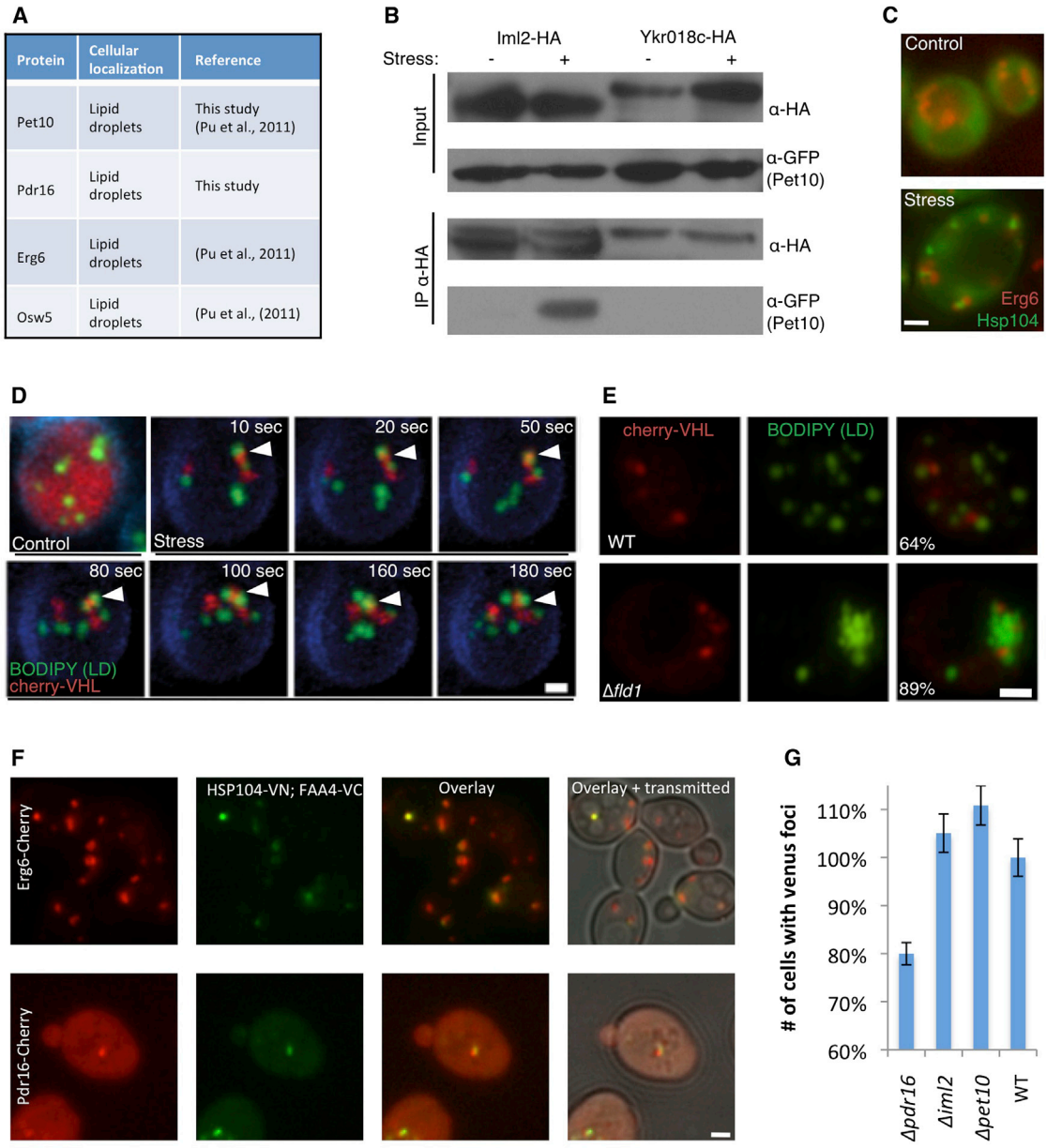

Figure 2. Inclusion Bodies and Lipid Droplets Are Juxtaposed in Cells

(A) Large-scale protein complementation assay performed for Iml2 at 37°C uncovered physical interaction with Pet10 and Pdr16. Previous reports support this interaction.

(B) Co-immunoprecipitation of Iml2 shows that Pet10 interacts with Iml2 but not its homolog Ykr018c, specifically under stress conditions.

(C) A strain expressing an IB marker (Hsp104-GFP) and a LD marker (Erg6-RFP) exposed to standard conditions and stress conditions (37°C for 90 min with MG132) reveals proximity between IBs and LDs during stress.

(D) Time-lapse series of cells expressing Cherry-VHL and Erg6-RFP under stress conditions shows that the proximity between IBs and LDs is stable over time (arrowhead).

(E) WT strain expressing cherry-VHL stained with BODIPY for LDs and exposed to heat stress and imaged using structured illumination microscopy (SIM) shows that IBs and LDs are found in close proximity. Δ*fld1*, which has a phenotype of clustered LDs, shows clumping of IBs together with the LDs. Numbers indicate percentage of IBs found in proximity to LDs in each strain.

(F) Strains harboring two halves of split Venus on Hsp104 (an IB resident) and Faa4 (a LD resident) show a focal signal that co-localizes with a subpopulation of Erg6-Cherry positive LDs. The Venus signal overlaps completely with a specific subset of LDs that are marked by Pdr16-Cherry.

(G) Quantification of Venus foci on populations in different deletion backgrounds shows that Δ*pdr16* has a significant reduction in proximity.

See also Figure S2.

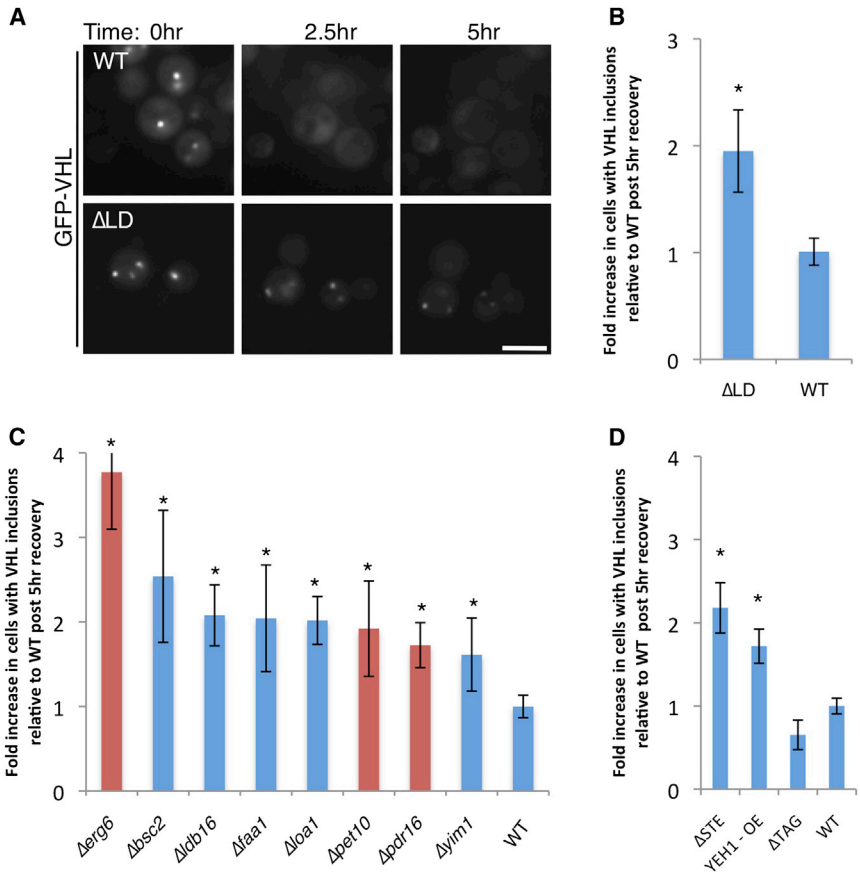

Figure 3. Lipid Droplets Are Crucial for the Efficient Clearance of Inclusion Bodies

(A) Images of a clearance assay in control (WT) and a quadruple deletion strain that lacks LDs (ΔLD), demonstrating that the ΔLD strain has a clearance defect.

(B) Quantification of the inclusion clearance defect in the ΔLD strain.

(C) Screening deletion strains of all LD proteins reveals that eight deletions phenocopy the inclusion clearance defect of the ΔLD strain. Red bars indicate Iml2 interactors shown in Figure 2A.

(D) Strains lacking steryl esters (STE) either by deletion of the biosynthesis enzymes (ΔSTE) or by overexpression of sterol-ester hydrolyzing enzyme (*YEH1 OE*) cause a defect in IB clearance (p value < 0.05). Deletion of the triacylglycerol biosynthesis enzymes (ΔTAG) had minimal effect on inclusion clearance. SE was calculated from three biological repeats (p value < 0.05). Scale bar, 5 μm.

See also Figure S3 and Tables S1 and S2.

We extracted total lipids and analyzed them by gas-chromatography mass spectrometry and found a near-identical lipid profile between conditions spanning hundreds of peaks. Only two, small, yet highly reproducible (three biologically independent experiments), differential peaks (at 588 and 604 s) appeared only under IB forming conditions (Figure 4A). These peaks could not be detected under identical conditions in the ΔSTE strain (Figure 4A), suggesting that STEs are needed for the biosynthesis of these molecules. Since these peaks were readily detectable on the background of Δ*iml2*, Δ*pet10*, and Δ*pdr16* it seems that these proteins do not affect the biosynthesis of these compounds (Figure 4B). Unfortunately, using mass spectrometry we could not identify the exact nature of these peaks, however, both have shared spectra of a sterol backbone with a hydroxyl and carbonyl groups (Figures 4A, left panel, and S3E), which could make them soluble enough to act as chemical chaperones.

We therefore tested if addition of a similar hydroxy-sterol could rescue the ΔSTE clearance phenotype. Indeed, 25-hydroxycholesterol could rescue the clearance defect of the ΔSTE strain (Figure 4C), in contrast to other studied chemical chaperones (proline [Chattopadhyay et al., 2004] and Tween-20 [Kreilgaard et al., 1998]) that did not have any effect on the clearance process in the WT or mutants (Figure 4D). Remarkably, the addition of 25-hydroxycholesterol to the Δ*iml2* strain did not improve clearance (Figure 4C), implying that Iml2 is necessary to enable access of the soluble sterol derivative to the IB.

Our work therefore suggests that a soluble sterol derivative, formed by STE and emanating from LDs, is important for efficient clearance of IBs and requires Iml2 to perform its role (Figure 4E). Since Iml2 is conserved, this process may very well occur also in mammals as we could show that in cell lines IBs and LDs are also found proximally (Figure S4A), are tethered (Figure S4B), and their proximity can be modulated by reducing the level of STEs using ACAT inhibitors (Figures S4C and S4D).

Previous reports provide additional examples of a close proximity between LDs and terminally misfolded protein compartments in mammals. For example, aggregates of Parkinson and Alzheimer disease-related proteins (α-synuclein and amyloid β-peptide), were shown to localize to LDs in neuronal cell culture (Cole et al., 2002) and patients (Gómez-Ramos and Asunción Morán, 2007). Additionally, the ER-associated degradation (ERAD) substrates, ApoB and HMG-CoA reductase, both accumulate on the surface of LDs following proteasome inhibition (Hartman et al., 2010; Ohsaki et al., 2006). Each of these examples focused on the unique properties of the substrate proteins as an explanation for their presence on LDs. Our observations were made by looking at a model substrate (VHL), which is cytosolic, has no transmembrane domains, no large hydrophobic domains or amyloidogenic properties. Together, our data argue for a general and conserved role of LDs in proteostasis.

In the past years, it is becoming clear that LDs are more then an energy storage depot and serve additional cellular functions (Walther and Farese, 2012; Welte, 2007). Here, we expand the role of LDs as a compartment that comes in contact with IBs and is actively involved in their clearance from the cytosol. The role of LDs in inclusion clearance may have medical implications for inclusion-related disorders, including some neurodegenerative conditions, which potentially could be targets for therapy.

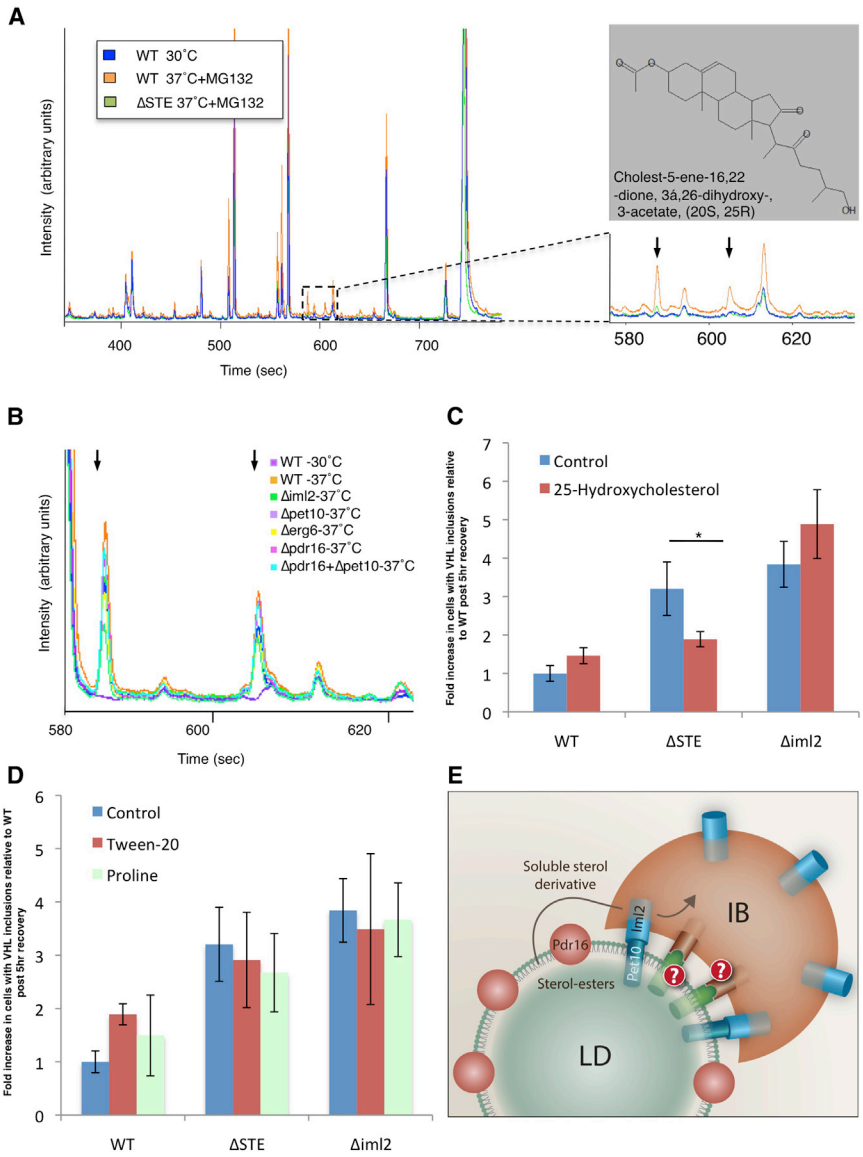

Figure 4. A Sterol Metabolite Is Involved in Inclusion Body Clearance

(A) Lipid profile of sterols extracted from either WT or ΔSTE strains grown at 30°C or exposed to stress conditions (37°C with proteasome inhibition) and subjected to GC-MS. Differential peaks are marked by arrows. The unidentified molecule has some shared mass spectra with Cholest-5-ene-16,22-dione, 3á,26-dihydroxy-, 3-acetate, (20S, 25R) See also Figure S3E.

(B) GC-MS lipid profile of mutant strains grown under stress conditions show a comparable profile to WT, suggesting that these mutants do not affect the synthesis of the sterol derivative.

(C) The presence of 25-hydroxycholesterol, soluble sterol, rescues the IB clearance defect of ΔSTE but not of Δ*iml2*.

(D) Clearance assays in the presence of the known chemical chaperones Proline and Tween-20 demonstrate no effect on IB clearance in either ΔSTE or Δ*iml2* strains.

(E) Schematic working model: IBs and LDs are in close proximity as observed by the physical interaction between Iml2 and Pet10. STE are precursors for biosynthesizing a soluble sterol derivative that is important for the clearance process and requires Iml2 for its function.

EXPERIMENTAL PROCEDURES

Yeast Strains and Libraries

All yeast transformation and library manipulation were preformed by standard protocols (see Supplemental Experimental Procedures for details).

Inclusion Body Clearance Assay

Deletion strains containing plasmids with *GFP-VHL* under galactose driving promoter were grown over night in 2% raffinose medium in a 96-plate (NUNC) and back-diluted 1:10 into 2% galactose media. Cells were incubated at 30°C for 3 hr and then exposed to inclusion forming conditions: MG132 (Calbiochem) was added to a final concentration of 80 μM, and cells were exposed to 37°C for 90 min in a PCR block. Fifty microliters from each strain were moved onto glass bottom 384-plate (Matrical Bioscience) covered with Concanavalin A (Sigma-Aldrich), washed twice with DDW followed by addition of 2% glucose media to shut off GFP-VHL induction. Time-lapse microscopy began immediately, acquiring images every hour at 22°C.

Analysis for inclusion clearance was done as follows: all images were viewed with the exact same contrast adjustments using ScanR analysis software (Olympus). The inclusion clearance score is the ratio between the number of cells with inclusion bodies at the 5-hr time point divided by the total number of GFP expressing cells at zero time point, which was counted by the ScanR software. To reduce the noise of this assay, the score for a given strain is always compared the value of the WT strain, which is assayed at that specific experiment. Data presented as fold change compared to the WT. For each strain, repetitions were conducted from three independent transformants.

Protein Complementation Assay Screen using the DHFR Library

Two Iml2 strains tagged with either half of the DHFR enzyme were picked from either the MATa or MATα DHFR libraries, and interaction analysis was performed as previously described (Tarassov et al., 2008) at 30°C and 37°C for 5 days. As a control for the specificity of the assay for Iml2, other inclusion residents found in our screen Mrn1 and Elp3, were screened in the same manner to ensure identification of specific Iml2 interactions (data not shown).

Lipid Analysis by Non-targeted Gas Chromatography-Mass Spectrometry

Lipids were extracted as previously described in the Bligh-dyer protocol (Bligh and Dyer, 1959). For additional details see Supplemental Information.

Structured Illumination Microscopy

Cells were seeded on concanavalin A-coated 35-mm plates (Ibidi). Prior to imaging, the point-spread function was visualized with 100 nm fluorescence beads. Images were acquired using Nikon nSIM microscope equipped with a 100× Apochromat TIRF oil objective (NA 1.49) in 3D mode. The raw data were examined for the grid pattern. Images were reconstructed with NIS-Elements software.

SUPPLEMENTAL INFORMATION

Supplemental Information includes Supplemental Experimental Procedures, four figures, and two tables and can be found with this article online at http://dx.doi.org/10.1016/j.devcel.2015.04.015.

ACKNOWLEDGMENTS

We wish to thank M. Breker and S. Chuartzman for their support with the high-content microscopy screens; P. Golubinoff for many exciting discussions; J. Lindberg Yilmaz (Prof. Sten Stymne's group) for generously providing the ΔLD, ΔSTE, and ΔTAG strains; T. Yuan Chang for his generous gift of ACAT inhibitor; and Z. Elazar, T. Ast, and E. Zalckavar for critical reading of the manuscript. This study was supported by ERC StG (260395) (M.S.), the generous support of the Kekst Family Institute for Medical Genetics (M.S.), Israel Science Foundation grant ISF 843/11 (D.K.), an ERC-StG2013 337713 DarkSide grant (D.K.), and a German Israel Foundation grant GIFI-1201-242.13/2012 (D.K.). M.S. is an EMBO Young Investigator and is supported by the Israel Ministry of Science.

Received: December 5, 2013
Revised: February 17, 2015
Accepted: April 21, 2015
Published: May 21, 2015

REFERENCES

Amen, T., and Kaganovich, D. (2015). Dynamic droplets: the role of cytoplasmic inclusions in stress, function, and disease. Cell. Mol. Life Sci. *72*, 401–415.

Bligh, E.G., and Dyer, W.J. (1959). A rapid method of total lipid extraction and purification. Can. J. Biochem. Physiol. *37*, 911–917.

Breker, M., Gymrek, M., and Schuldiner, M. (2013). A novel single-cell screening platform reveals proteome plasticity during yeast stress responses. J. Cell Biol. *200*, 839–850.

Chattopadhyay, M.K., Kern, R., Mistou, M.Y., Dandekar, A.M., Uratsu, S.L., and Richarme, G. (2004). The chemical chaperone proline relieves the thermosensitivity of a dnaK deletion mutant at 42 degrees C. J. Bacteriol. *186*, 8149–8152.

Cohen, Y., and Schuldiner, M. (2011). Advanced methods for high-throughput microscopy screening of genetically modified yeast libraries. Methods Mol. Biol. *781*, 127–159.

Cohen, E., Bieschke, J., Perciavalle, R.M., Kelly, J.W., and Dillin, A. (2006). Opposing activities protect against age-onset proteotoxicity. Science *313*, 1604–1610.

Cole, N.B., Murphy, D.D., Grider, T., Rueter, S., Brasaemle, D., and Nussbaum, R.L. (2002). Lipid droplet binding and oligomerization properties of the Parkinson's disease protein alpha-synuclein. J. Biol. Chem. *277*, 6344–6352.

de Almeida, S.F., Picarote, G., Fleming, J.V., Carmo-Fonseca, M., Azevedo, J.E., and de Sousa, M. (2007). Chemical chaperones reduce endoplasmic reticulum stress and prevent mutant HFE aggregate formation. J. Biol. Chem. *282*, 27905–27912.

Escusa-Toret, S., Vonk, W.I., and Frydman, J. (2013). Spatial sequestration of misfolded proteins by a dynamic chaperone pathway enhances cellular fitness during stress. Nat. Cell Biol. *15*, 1231–1243.

Gardner, R.G., Nelson, Z.W., and Gottschling, D.E. (2005). Degradation-mediated protein quality control in the nucleus. Cell *120*, 803–815.

Gómez-Ramos, P., and Asunción Morán, M. (2007). Ultrastructural localization of intraneuronal Abeta-peptide in Alzheimer disease brains. J. Alzheimers Dis. *11*, 53–59.

Hartman, I.Z., Liu, P., Zehmer, J.K., Luby-Phelps, K., Jo, Y., Anderson, R.G., and DeBose-Boyd, R.A. (2010). Sterol-induced dislocation of 3-hydroxy-3-methylglutaryl coenzyme A reductase from endoplasmic reticulum membranes into the cytosol through a subcellular compartment resembling lipid droplets. J. Biol. Chem. *285*, 19288–19298.

Haslbeck, M., Miess, A., Stromer, T., Walter, S., and Buchner, J. (2005). Disassembling protein aggregates in the yeast cytosol. The cooperation of Hsp26 with Ssa1 and Hsp104. J. Biol. Chem. *280*, 23861–23868.

Hill, S.M., Hao, X., Liu, B., and Nyström, T. (2014). Life-span extension by a metacaspase in the yeast Saccharomyces cerevisiae. Science *344*, 1389–1392.

Huh, W.K., Falvo, J.V., Gerke, L.C., Carroll, A.S., Howson, R.W., Weissman, J.S., and O'Shea, E.K. (2003). Global analysis of protein localization in budding yeast. Nature *425*, 686–691.

Kaganovich, D., Kopito, R., and Frydman, J. (2008). Misfolded proteins partition between two distinct quality control compartments. Nature *454*, 1088–1095.

Karplus, K. (2009). SAM-T08, HMM-based protein structure prediction. Nucleic Acids Res. *37*, W492–W497.

Koenig, U., Fobker, M., Lengauer, B., Brandstetter, M., Resch, G.P., Groger, M., Plenz, G., Pammer, J., Barresi, C., Hartmann, C., et al. (2015). Autophagy facilitates secretion and protects against degeneration of the harderian gland. Autophagy *11*, 298–313.

Köffel, R., Tiwari, R., Falquet, L., and Schneiter, R. (2005). The Saccharomyces cerevisiae YLL012/YEH1, YLR020/YEH2, and TGL1 genes encode a novel family of membrane-anchored lipases that are required for steryl ester hydrolysis. Mol. Cell. Biol. *25*, 1655–1668.

Kopito, R.R. (2000). Aggresomes, inclusion bodies and protein aggregation. Trends Cell Biol. *10*, 524–530.

Kreilgaard, L., Jones, L.S., Randolph, T.W., Frokjaer, S., Flink, J.M., Manning, M.C., and Carpenter, J.F. (1998). Effect of Tween 20 on freeze-thawing- and agitation-induced aggregation of recombinant human factor XIII. J. Pharm. Sci. *87*, 1597–1603.

Kuang, W.W., Thompson, D.A., Hoch, R.V., and Weigel, R.J. (1998). Differential screening and suppression subtractive hybridization identified genes differentially expressed in an estrogen receptor-positive breast carcinoma cell line. Nucleic Acids Res. *26*, 1116–1123.

Li, D., Song, J.Z., Li, H., Shan, M.H., Liang, Y., Zhu, J., and Xie, Z. (2015). Storage lipid synthesis is necessary for autophagy induced by nitrogen starvation. FEBS Lett. *589*, 269–276.

Malinovska, L., Kroschwald, S., Munder, M.C., Richter, D., and Alberti, S. (2012). Molecular chaperones and stress-inducible protein-sorting factors coordinate the spatiotemporal distribution of protein aggregates. Mol. Biol. Cell *23*, 3041–3056.

McCammon, M.T., Hartmann, M.A., Bottema, C.D., and Parks, L.W. (1984). Sterol methylation in Saccharomyces cerevisiae. J. Bacteriol. *157*, 475–483.

McClellan, A.J., Scott, M.D., and Frydman, J. (2005). Folding and quality control of the VHL tumor suppressor proceed through distinct chaperone pathways. Cell *121*, 739–748.

Ogrodnik, M., Salmonowicz, H., Brown, R., Turkowska, J., Średniawa, W., Pattabiraman, S., Amen, T., Abraham, A.C., Eichler, N., Lyakhovetsky, R., and Kaganovich, D. (2014). Dynamic JUNQ inclusion bodies are asymmetrically inherited in mammalian cell lines through the asymmetric partitioning of vimentin. Proc. Natl. Acad. Sci. USA *111*, 8049–8054.

Ohsaki, Y., Cheng, J., Fujita, A., Tokumoto, T., and Fujimoto, T. (2006). Cytoplasmic lipid droplets are sites of convergence of proteasomal and autophagic degradation of apolipoprotein B. Mol. Biol. Cell *17*, 2674–2683.

Parsell, D.A., Kowal, A.S., Singer, M.A., and Lindquist, S. (1994). Protein disaggregation mediated by heat-shock protein Hsp104. Nature *372*, 475–478.

Pettersen, E.F., Goddard, T.D., Huang, C.C., Couch, G.S., Greenblatt, D.M., Meng, E.C., and Ferrin, T.E. (2004). UCSF Chimera—a visualization system for exploratory research and analysis. J. Comput. Chem. *25*, 1605–1612.

Pfisterer, S.G., Bakula, D., Cezanne, A., Robenek, H., and Proikas-Cezanne, T. (2014). WIPI β-propellers at the crossroads of autophagosome and lipid droplet dynamics. Biochem. Soc. Trans. *42*, 1414–1417.

Pu, J., Ha, C.W., Zhang, S., Jung, J.P., Huh, W.K., and Liu, P. (2011). Interactomic study on interaction between lipid droplets and mitochondria. Protein Cell *2*, 487–496.

Ren, J., Pei-Chen Lin, C., Pathak, M.C., Temple, B.R., Nile, A.H., Mousley, C.J., Duncan, M.C., Eckert, D.M., Leiker, T.J., Ivanova, P.T., et al. (2014). A phosphatidylinositol transfer protein integrates phosphoinositide signaling with lipid droplet metabolism to regulate a developmental program of nutrient stress-induced membrane biogenesis. Mol. Biol. Cell *25*, 712–727.

Sandager, L., Gustavsson, M.H., Ståhl, U., Dahlqvist, A., Wiberg, E., Banas, A., Lenman, M., Ronne, H., and Stymne, S. (2002). Storage lipid synthesis is non-essential in yeast. J. Biol. Chem. *277*, 6478–6482.

Spang, N., Feldmann, A., Huesmann, H., Bekbulat, F., Schmitt, V., Hiebel, C., Koziollek-Drechsler, I., Clement, A.M., Moosmann, B., Jung, J., et al. (2014). RAB3GAP1 and RAB3GAP2 modulate basal and rapamycin-induced autophagy. Autophagy *10*, 2297–2309.

Specht, S., Miller, S.B., Mogk, A., and Bukau, B. (2011). Hsp42 is required for sequestration of protein aggregates into deposition sites in Saccharomyces cerevisiae. J. Cell Biol. *195*, 617–629.

Spokoini, R., Moldavski, O., Nahmias, Y., England, J.L., Schuldiner, M., and Kaganovich, D. (2012). Confinement to organelle-associated inclusion structures mediates asymmetric inheritance of aggregated protein in budding yeast. Cell Rep. *2*, 738–747.

Sung, M.K., and Huh, W.K. (2007). Bimolecular fluorescence complementation analysis system for in vivo detection of protein-protein interaction in Saccharomyces cerevisiae. Yeast *24*, 767–775.

Szymanski, K.M., Binns, D., Bartz, R., Grishin, N.V., Li, W.P., Agarwal, A.K., Garg, A., Anderson, R.G., and Goodman, J.M. (2007). The lipodystrophy protein seipin is found at endoplasmic reticulum lipid droplet junctions and is important for droplet morphology. Proc. Natl. Acad. Sci. USA *104*, 20890–20895.

Tarassov, K., Messier, V., Landry, C.R., Radinovic, S., Serna Molina, M.M., Shames, I., Malitskaya, Y., Vogel, J., Bussey, H., and Michnick, S.W. (2008). An in vivo map of the yeast protein interactome. Science *320*, 1465–1470.

Teslovich, T.M., Musunuru, K., Smith, A.V., Edmondson, A.C., Stylianou, I.M., Koseki, M., Pirruccello, J.P., Ripatti, S., Chasman, D.I., Willer, C.J., et al. (2010). Biological, clinical and population relevance of 95 loci for blood lipids. Nature *466*, 707–713.

Tong, A.H., and Boone, C. (2006). Synthetic genetic array analysis in Saccharomyces cerevisiae. Methods Mol. Biol. *313*, 171–192.

van den Hazel, H.B., Pichler, H., do Valle Matta, M.A., Leitner, E., Goffeau, A., and Daum, G. (1999). PDR16 and PDR17, two homologous genes of Saccharomyces cerevisiae, affect lipid biosynthesis and resistance to multiple drugs. J. Biol. Chem. *274*, 1934–1941.

Walther, T.C., and Farese, R.V., Jr. (2012). Lipid droplets and cellular lipid metabolism. Annu. Rev. Biochem. *81*, 687–714.

Weisberg, S.J., Lyakhovetsky, R., Werdiger, A.C., Gitler, A.D., Soen, Y., and Kaganovich, D. (2012). Compartmentalization of superoxide dismutase 1 (SOD1G93A) aggregates determines their toxicity. Proc. Natl. Acad. Sci. USA *109*, 15811–15816.

Welte, M.A. (2007). Proteins under new management: lipid droplets deliver. Trends Cell Biol. *17*, 363–369.